Real-time Clock Estimation for Precise Orbit Determination of LEO-Satellites

A. Hauschild, O. Montenbruck
Deutsches Zentrum für Luft- und Raumfahrt (DLR), German Space Operations Center (GSOC), Germany

BIOGRAPHY

André Hauschild is a PhD candidate at German Space Operations Center (GSOC). His current activities focus on real-time estimation of GPS satellite clocks. He received his diploma in mechanical engineering from Technical University at Braunschweig, Germany.

Dr. Oliver Montenbruck is head of the GPS Technology and Navigation Group at GSOC. His current field of work comprises the development of on-board navigation systems and spaceborne GPS applications. He has written various text books on computational astronomy and satellite orbits. He received his PhD from University of Technology at Munich, Germany.

ABSTRACT

In this paper, a real-time system for clock offset estimation of GPS satellites is presented. The algorithm is based on a Kalman-filter and processes undifferenced code and carrier-phase measurements of a global NTRIP tracking network. The clock offset and drift of the satellite clocks are estimated along with tracking station clock offsets, tropospheric zenith path delay and carrier-phase ambiguities. The filter algorithm and data processing scheme is presented. The accuracy of the orbit and clock product is assessed with a precise orbit determination of the TerraSar-X satellite and compared to results gained with the IGU predicted products.

INTRODUCTION

A growing number of near real-time precise point positioning (PPP) applications raises the need for precise GPS orbit and clock products with short latency. One of these applications is the precise orbit determination (POD) of low-earth-orbit satellites. The mission objectives for many current and future missions require the satellite orbit to be determined shortly after the ground station pass, because it is needed for further processing the data of the satellite's payloads. The observations of the satellite's GPS receiver are available immediately after the download to the ground station. Positioning also requires precise orbit and clock data for the complete GPS constellation. The rubidium and cesium atomic standards of the GPS satellites are subject to clock noise and frequency variations, which can originate from a variety of effects and are hard to forecast. Predictions of clock offset and drift, which are provided for example in the predicted part of the IGS ultra-rapid orbits or the broadcast ephemerides, deviate quickly from the true values by several decimeters or even meters. Thus these orbit/clock-products become unusable for PPP applications, where a carrier-phase based positioning accuracy down to centimeter level is desired. The solution to this problem is the use of clock offsets, which have been estimated from GPS measurements originating from a network of sensor stations. Currently, only a limited set of providers for precise (near-) real-time orbit/clock-products is available. Among them are three of the IGS Analysis Centers: JPL [1], NRCan and ESA [2]. The JPL products are a commercial product and are transmitted to the user with a latency of about 5 seconds. They can be accessed in various ways, for example internet data streams and satellite broadcast. The real-time orbit and clock products from ESA and NRCan are currently generated in the context of the IGS real-time pilot project, but not publicly available.

A real-time system for clock estimation (RETICLE) is currently under development at German Space Operations Center of DLR. The generated orbit/clock-products will be used to support orbit determination of low-earth-orbit

(LEO) satellites for up-coming space missions, which require near real-time orbit determination accuracies down to 8-10 cm. The software is based on a Kalman-Filter, which processes undifferenced code and carrier phase observations from a worldwide network of GPS stations. The filter uses the orbit information from the predicted part of the latest ultra-rapid IGS products, and estimates clock offsets and drifts for the complete GPS constellation. In this paper, the complete filter algorithm including the pre-processing of the raw measurements is introduced. The orbit and clock products computed with the filter algorithm are used for a precise orbit determination with real GPS measurements from the receiver on board the TerraSar-X (TSX) satellite. The same analysis is also performed with the IGS ultra-rapid products and the results are compared and discussed.

CLOCK ESTIMATION WITH RETICLE

The real-time clock-estimation system (RETICLE) comprises a Kalman-filter, which is the core algorithm of the system, together with several functions, which handle the retrieval of measurement and auxiliary data. In this section, an overview of the system will be provided, followed by a detailed description of the GPS measurement pre-processing procedure and the Kalman filter layout. Fig. 1 provides an overview of the complete system.

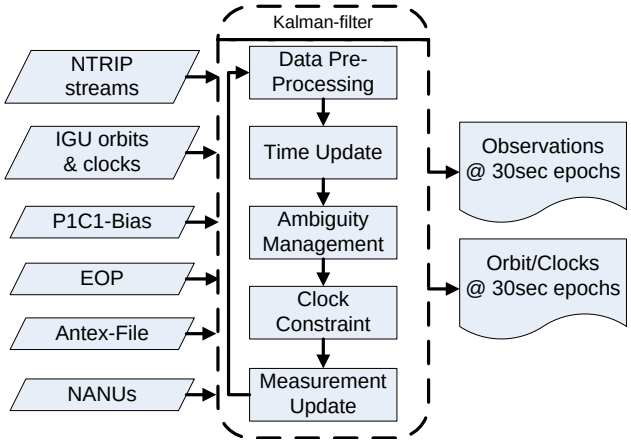

Fig. 1 Overview of the RETICLE-System

The Kalman filter processes measurements received from a global network of GPS reference stations. These stations transmit their observations in real-time as NTRIP data-streams [3]. The RETICLE-system can use data-streams provided in RTCM2, RTCM3 and RTIGS format, which are the three major formats in the NTRIP network. Fig. 2 shows a map with the real-time stations used for the generation of the clock product presented in this paper. The colorscale indicates the amount of stations which can track a GPS satellite simultaneously. Whereas the coverage in the areas around North America, Europe and Australia is highly redundant, the pacific ocean and smaller areas in Africa and Asia exhibit low coverage with only 4 or 5 stations per satellite. The data streams contain dual frequency observations at a data rate of 1 Hz. Measurements at 30 second epochs are stored in an internal buffer for access by the Kalman filter and additionally recorded in Rinex-files.

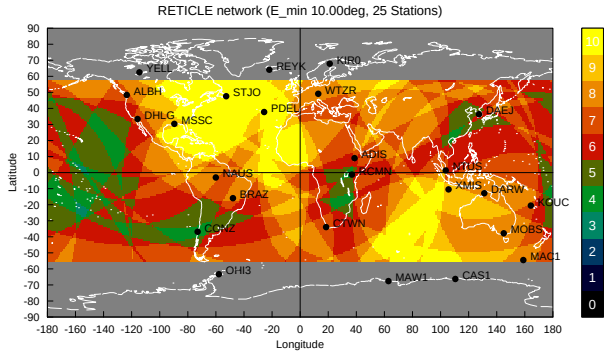

Fig. 2 Global NTRIP real-time station network used for RETICLE, the colorcode indicates the amount of stations simultaneously visible by a GPS satellite

The predicted part of the IGS ultra-rapid (IGU) orbits and clocks is used as a-priori information during data-preprocessing. The orbits are currently updated four times each day at 3 h, 9 h, 15 h and 21 h UTC and have a latency of 3 hours relative to the last observations. Since the accuracy of the predicted orbits and especially the clocks degrades with an increasing age of data, the most recent product should be used as soon as it becomes available. Therefore, the IGU orbits are downloaded and concatenated at 3 h, 9 h, 15 h and 21 h, respectively. Additionally, a cosine-weighted interpolation is used to fade-out the old orbit, and clock and fade-in the new product. Thereby, discontinuities are reduced.

The differential code bias corrections for the P1-code and the C/A-code must be used since approximately 60% of the stations do not transmit the P1-code observable due to receiver or stream-format limitations. The ionosphere-free combination is then formed from C/A and P2 observations instead of P1 and P2. A correction for the C1P1-bias must be applied in order to assure consistent processing of all observations. Since the biases change slowly, the correction values are only updated weekly and retreived from the Center of Orbit Determination in Eurpe (CODE) [4].

Furthermore, the most recent predicted earth-orientation-parameters (EOP) from the IGS are downloaded daily from the IGS. The most recent antenna phase center offsets (PCO) and variations (PCV) according to the IGS05-convention are used for the computation of the RETICLE-clocks. For precise positioning, the phase center of an antenna can no longer be defined as a fixed point, because elevation- and azimuth-dependent phase reception patterns must be taken into account. Therefore, each GPS antenna is characterized using a constant phase center offset vector and a table, which holds the information for the phase reception pattern. The data for all GPS satellite

antennas and reference station antennas is provided as an Antex-file by the IGS [5].

Finally, up-to-date information about the current status of the GPS constellation must also be present in the RETICLE system. Satellites are frequently set unusable due to orbital maneuvers or maintenance and must be excluded from the clock estimation during these periods. The information about the planned maneuvers and maintenance is obtained form the most recent Notice Advisory to Navstar Users (NANUs), which are downloaded and processed every hour.

All of these auxiliary processes described previously are automated and do not require user interactions. The only exception is the update of the Antex-file, which occurs once or twice a year and must be performed manually.

Fig. 1 depicts also a flowchart of the Kalman-filter algorithm. The filter state includes the satellite clock error $dt^{(s)}$ and the clock drift $df^{(s)}$ for the complete constellation of 32 satellites. In the notation adapted for this paper, the superscript (s) stands for the index of the GPS satellite. The state vector additionally comprises the receiver clock offset dt_n, a differential tropospheric zenith delay dT_n as well as the float carrier phase ambiguities $N_{n,i}$ for all satellites in view of each station. In our notation the subscript n denotes the individual tracking station and i denotes the i-th satellite tracked by the station. The current GPS constellation has 30 active satellites and the typical tracking network size for the filter is about 25 stations. The assumption that each station tracks on average 10 GPS satellites leads to a total number of about 300 elements in the state vector.

Some of the state vector elements require further explanation: The estimated satellite clock offset and drift are computed with respect to the GPS time scale. The receiver clock offsets for the tracking stations, however, do not represent the offset of the real receiver clocks, since the observations have been pre-processed before being used in the filter. The pseudorange observations are used together with the a-priori orbits and the known station position to compute a coarse estimation of the receiver's clock error. All observations and the measurement epoch are then corrected by the estimated clock offset. This pre-processing is necessary to reduce large clock jumps in the order of milliseconds to less then a microsecond, which can easily be compensated by process noise in the Kalman filter.

The estimated differential tropospheric zenith delay shall also be explained in further detail here. The model of the ionosphere-free code and carrier phase observables already includes corrections for the tropospheric delay using a model of the standard atmosphere, which will be introduced later in this section. The true tropospheric delay, however, will differ from the values provided by the empirical model, since the actual local weather conditions deviate from the model parameters. To compensate these deviations, the differential zenith path delay dT_n is estimated for each station, which is then mapped into a differential tropospheric slant delay, using an elevation dependent mapping function. The carrier phase ambiguities in the filter state are estimated as float values and are not fixed. The state vector $\boldsymbol{x}$ can now be written as

$$\boldsymbol{x} = \begin{bmatrix} (dt^{(1)} & \dots & dt^{(32)})^T \\ (df^{(1)} & \dots & df^{(32)})^T \\ (dt_1 & \dots & dt_n)^T \\ (dT_1 & \dots & dT_n)^T \\ (N_{1,1} & \dots & N_{1,12})^T \\ \vdots & & \vdots \\ (N_{1,1} & \dots & N_{1,12})^T \end{bmatrix} \tag{1}$$

In order to be able to perform the Kalman-filter time update, the state vector must be predicted towards the next update epoch using a system model. For this algorithm, the GPS satellite clocks are predicted linearly in time. The clock drift and all other state parameters are assumed to be constant. The state transition matrix required for the time update of the filter state is therefore simplified to:

$$\boldsymbol{\Phi} = \begin{bmatrix} \boldsymbol{I}_{32,32} & \boldsymbol{I}_{32,32}\Delta t & \mathbf{0}_{32,14n} \\ \mathbf{0}_{32,32} & \boldsymbol{I}_{32,32} & \mathbf{0}_{32,14n} \\ \mathbf{0}_{14n,32} & \mathbf{0}_{14n,32} & \boldsymbol{I}_{14n,14n} \end{bmatrix} \tag{2}$$

In this matrix notation, $\boldsymbol{I}$ denotes a unit matrix and $\mathbf{0}_{i,j}$ is a zero matrix with i rows and j columns. The term Δt is the time step between two filter updates.

Of course, the satellite clock drift is not strictly constant, but it undergoes slow variations. These variations are due to the characteristics of the individual satellite clocks and are driven by hardly predictable effects like thermal variations on board the GPS satellites. Furthermore, the ground station clock offsets and the differential tropospheric delays are subject to variations. In order to compensate these deviations of the system model from the truth, process noise is introduced on the corresponding elements of the state vector. Without process noise, the covariance of the state vector would decrease over time and as a result, the weight of the measurements during the filter update decreases, which leads to divergence of the filter.

The state transition matrix is used to propagate the state vector as well as the covariance matrix :

$$\boldsymbol{x}_{k+1} = \boldsymbol{\Phi}\boldsymbol{x}_k \tag{3}$$

$$\boldsymbol{P}^-_{k+1} = \boldsymbol{\Phi}\boldsymbol{P}\boldsymbol{\Phi}^T + \boldsymbol{Q} \tag{4}$$

The increment in process noise is assumed to result from an integrated white noise process, or random walk process, and the associated covariance grows linearly in time. For simplicity, the matrix $\mathbf{Q}dt$ is assumed to be a diagonal matrix of the following form:

$$\boldsymbol{Q} = \begin{bmatrix} \frac{\sigma^2_{dt}\Delta t}{\tau_{dt}}\boldsymbol{I}_{32} & \mathbf{0} & \mathbf{0} & \mathbf{0} & \mathbf{0} \\ \mathbf{0} & \frac{\sigma^2_{df}\Delta t}{\tau_{df}}\boldsymbol{I}_{32} & \mathbf{0} & \mathbf{0} & \mathbf{0} \\ \mathbf{0} & \mathbf{0} & \frac{\sigma^2_{dt_n}\Delta t}{\tau_{dt_n}}\boldsymbol{I}_n & \mathbf{0} & \mathbf{0} \\ \mathbf{0} & \mathbf{0} & \mathbf{0} & \frac{\sigma^2_{dT_n}\Delta t}{\tau_{dT_n}}\boldsymbol{I}_n & \mathbf{0} \\ \mathbf{0} & \mathbf{0} & \mathbf{0} & \mathbf{0} & \mathbf{0} \end{bmatrix} \tag{5}$$

The process noise is characterized using the standard deviation σ and a time constant τ.

Special care has been taken in modeling the pseudorange and carrier phase observations. The position vector of the ground station $\boldsymbol{r}_n$ in the earth-centered earth-fixed (ECEF) coordinate frame is obtained from recent IGS-Sinex files. The variations of the station position due to solid earth tides, pole tides and ocean loading are also included in the modeling of $\boldsymbol{r}_n$ [6]. The ionosphere-free combination of pseudorange and carrier phase, ρ_{IF} and Φ_{IF}, respectively, are formed according to:

$$\rho_{IF} = \frac{f_{L1}^2}{f_{L1}^2 - f_{L2}^2}\rho_{L1} - \frac{f_{L2}^2}{f_{L1}^2 - f_{L2}^2}\rho_{L2} \tag{6}$$

$$\Phi_{IF} = \frac{f_{L1}^2}{f_{L1}^2 - f_{L2}^2}\Phi_{L1} - \frac{f_{L2}^2}{f_{L1}^2 - f_{L2}^2}\Phi_{L2} \tag{7}$$

where f_{L1} and f_{L2} are the L1 and L2 frequencies and ρ_{L1}, ρ_{L2}, Φ_{L1} and Φ_{L2} are the corresponding pseudorange and carrier phase observables. The modelling equations for ρ_{IF} and Φ_{IF} are:

$$\begin{aligned}\rho_{IF} &= |\boldsymbol{r}^{(s)} - \boldsymbol{r}_n| + c\left(dt^{(s)} - dt_n\right) + cdt_{rel} + T_n \\ &\quad + MdT_n + b_{P1C1} + b_{PCO} + b_{PCV} \qquad (8)\\ \Phi_{IF} &= |\boldsymbol{r}^{(s)} - \boldsymbol{r}_n| + c\left(dt^{(s)} - dt_n\right) + cdt_{rel} + T_n \\ &\quad + MdT_n + b_{PWU} + b_{PCO} + b_{PCV} - N_n^{(s)} \qquad (9)\end{aligned}$$

In Eq. 8 and Eq. 9, $\boldsymbol{r}^{(s)}$ is the position vector of the GPS satellite and $\boldsymbol{r}_n$ is the position vector of the ground station antenna reference point. The speed of light is denoted with c. The satellite clock offset $dt^{(s)}$ and the receiver clock offset dt_n have already been introduced as elements of the state vector. The correction term due to relativistic effects dt_{rel} consists of two components. The first component accounts for the periodic change in the GPS satellite clock rate as the satellites trajectory varies its nominal circular orbit. The second part is due to the space-time curvature correction.

The tropospheric path delay T_n is computed using the UNB3 model, which describes the signal transmission delay based on user position, time and elevation angle without the need for meteorological data [7]. The additional tropospheric zenith path delay dT_n is estimated in the state vector for each station. It is multiplied with an elevation dependent mapping function M in the observation model.

A P1-C1 differential code bias correction term b_{P1C1} is used for modeling the pseudorange observation in Eq. 8 in case the receiver does not provide P1-observations or uses cross-correlation tracking and reports a modified P2-observation. Finally, corrections due to phase center offset and phase center variations, dentoted b_{PCO} and b_{PCV}, respectively, are used to correct the transmitting (satellite) antenna and the receiving (station) antenna. The modeling of the ionosphere-free carrier phase observations also comprises the phase wind-up correction b_{PWU}. It is due to the phase wind-up phenomenon of a circular-polarized electromagnetic wave, which manifests itself in an apparent change in the observed carrier phase, if the transmitting or receiving antennas are rotating about their boresight vectors with respect to each other [8]. In this application, the receiving antennas are of course fixed in the earth-fixed frame, but the GPS satellite slowly changes its attitude to keep the solar panels pointed to the sun. It should be noted at this point that the same attitude model used for generating the orbit/clock product must also be used in the positioning application to ensure consistency of the phase windup corrections. Finally, the carrier phase ambiguity $N_n^{(s)}$ is also included in Eq. 9 and estimated as a float value in the state vector.

Upon initialization of the filter, the coarse values from the IGS ultra-rapid product are used as a-priori values for the satellite clock offset and drift. All other elements of the state vector are set to zero. The initial covariance matrix is set up as a diagonal matrix with the square of the initial standard deviation on the main diagonal.

In the following, a few remarks on the selection of the filter parameters are be added. The selection of the process noise and measurement noise determines whether the filter puts more weight on the propagated state based on the system model or on the actual measurements. That is, if the process noise is low compared to the measurement noise, the filter will rely more on the system model and will only gradually correct the filter state during the measurement update. Meaningful settings for the noise of the observables can easily be found from an assessment of the measurement precision. The carrier phase observables have been assigned a measurement noise of 2 cm. This value also takes the effect of possible multipath errors at a cutoff angle of 10 ° into account. The code observables have been weighted with a variance of 2 m.

The process noise of the elements in the state vector is in general more difficult to determine. Theoretically, the amount of phase and frequency process noise can be found from the Hadamard variance obtained from a clock characterization for each individual satellite clock [9]. A simplified approach has been chosen here to avoid this elaborate procedure. No distinction is made between the individual clocks. Instead the process noise settings are the same for all GPS satellites. In order to avoid filter divergence, process noise with a standard deviation of 3 centimeter and a time-constant of 600 minutes has been assigned to the clock offset parameter. The clock drift process noise has a standard deviation of 0.0005 m/s (≈10-12 s/s) over 900 s. The differential zenith path delays of the ground stations are assumed to vary only marginally over time. Consequently, only a small amount of process noise with a standard deviation of 2 mm over 1 hour is assigned. On the contrary, the ground station clock offset will exhibit noise-like behavior with deviations in the order of tens of meters due to the "clock-jump" elimination procedure mentioned previously. Therefore, the comparably large process noise

has been chosen to compensate for these deviations. The ambiguities of the carrier phase measurements are assumed to be constant parameters and therefore no process noise is introduced. The settings for the initial covariance matrix, the process noise and the measurement noise are summarized in Tab. 1.

Table 1 Filter settings for RETICLE Kalman-filter

Process Noise:	a priori	σ	τ
GPS clock offset	5 m	0.03 m	600 s
GPS clock drift	0.005 m	0.0005 m/s	900 s
Rcv clock offset	100 m	100 m	100 s
Tropospheric zenith delay	0.5 m	0.002 m	3600 s
Ambiguities	6 m	-	-
Measurement Noise:			
Pseudorange		2.0 m	
Carrier Phase		0.02 m	
Clock Constraint		0.1 m	
Edit Limits:			
Elevation	10 °		
Code-Carrier-Difference	10 m		
Pseudorange RMS	5 m		
Carrierphase RMS	0.04 m		

The Kalman-filter estimation loop depicted in Fig. 1 starts with the pre-processing of all observation collected at the epoch. During pre-processing, the ground station clock jumps are eliminated from the data as previously explained. The observables are screened for missing data and satellites which have dropped below an elevation cutoff angle of 10°. Additionally, the time difference of code-carrier differences is examined to eliminate large cycle slips. The core part of the data screening is an integrity monitoring, which is performed on the pseudorange and the carrier phase measurements in order to detect and remove outliers. During this monitoring, the orbits and clocks of the predicted IGU product are used together with the known station position to compute the residuals of the ionosphere-free observations for each satellite. Since the position is known, only the station clock offset, which is common for all measurements, must be computed and removed from the residuals. If the RMS of the pseudoranges exceeds a predefined threshold, the residuals are recursively recomputed with a single satellite excluded at a time. The combination, which yields the lowest residual, identifies the satellite with the outlier in the pseudorange measurement and this satellite is then excluded from the filter at this epoch. If the residual-threshold is still exceeded, the procedure of recursively excluding satellite is repeated until the threshold is met or the number of valid satellites drops to two. In the latter case, all remaining satellites are rejected as well, since the monitoring procedure cannot further be performed. A similar approach has been chosen for the monitoring and screening of the carrier phase measurements, but instead time differences of the carrier phases between the current and the previous epoch are used, in order to avoid the complication of handling ambiguities at this step. With this monitoring procedure, measurement outliers and cycle slips can be detected, and the associated satellites are excluded from the measurement update.

After the pre-processing of the observations, the filter state and the covariance matrix are propagated from the last epoch to the current epoch using Eq. 3 and Eq. 4. Afterwards, the ambiguities in the state vector are examined. If satellites have dropped below the elevation limit of the filter or are no longer tracked, their ambiguities are deleted and the space in the filter state is freed. If satellites are newly acquired, their ambiguities are initialized using code-carrier differences to provide their initial values. Also, ambiguities of satellites which have been rejected during the data screening are removed from the filter and initialized again as soon as valid measurements for the satellite are available. Prior to the measurement update, the filter applies a clock constraint, which is necessary to tie the clock correction values to the GPS timescale. For this purpose, a "pseudo"-measurement update is performed, which treats the mean of all clock offsets in the IGU clock product as observation of the mean clock offset in the filter state. Omitting the constraint can lead to a common offset of the clocks of the complete GPS constellation. This offset can be compensated in the estimated station clock offsets. It is thus unobservable in the conventional measurement update and must be constrained. The measurement update of the filter is typically performed 4 seconds after the measurements epoch, to provide an appropriate latency for the real-time data to arrive. A complete Kalman-filter cycle takes about 2.5 seconds on average, which means that the clock-estimates are available with a delay of 6.5 seconds. However, if these products are transmitted to external users, additional transport delays occur. The clock products are logged in a daily SP3 file. For near real-time orbit determination, a copy of the most recent SP3 file can be extracted from the system at any time. Additionally, the satellite positions and clock offsets can be transmitted via a TCP/IP-connection to users every 30 seconds.

ACCURACY ASSESSMENT OF CLOCK PRODUCTS

This section introduces the evaluation strategy of the orbit- and clock-products. The Signal-In-Space Range Error (SISRE) is used to provide a coarse estimate of the expected positioning accuracy [10]. The traditional SISRE equation has been modified for the analysis of this paper, to avoid that radial orbit offsets or clock errors, which are common to all satellites in the constellation, affect the computed SISRE value. In a navigation solution, these common errors would be absorbed into the receiver's clock correction values and do not affect the position. Therefore, the mean values of the orbit and clock errors of the complete constellation at the same epoch must be eliminated from the SISRE. The combined error of the radial orbit error and the clock offset error is found from $e_{RC} = e_R - e_{cdt}$. De-

noting the mean pseudorange errors over the complete constellation at each epoch with $\bar{e}_{RC}$, the corrected range error can be found as $\tilde{e}_{RC} = e_{RC} - \bar{e}_{RC}$. The modified SISRE equation for a single satellite i is

$$\mathrm{SISRE}^{(\mathrm{i})} = \sqrt{\mathrm{rms}\left(\tilde{\mathrm{e}}_{\mathrm{RC}}^{(\mathrm{i})}\right)^2 + \frac{1}{49}\left(\mathrm{rms}\left(\mathrm{e}_{\mathrm{C}}^{(\mathrm{i})}\right)^2 + \mathrm{rms}\left(\mathrm{e}_{\mathrm{A}}^{(\mathrm{i})}\right)^2\right)} \quad (10)$$

with the cross-track and along-track orbit errors e_C and e_A, respectively. In this equation the $\mathrm{rms}\,()$-terms denote the values of many individual orbit and clock errors over the time interval of interest. Finally, the first term in Eq. 10 can be replaced by e_R, which leaves only the radial, cross-track and along-track error components. This formulation is useful to assess the accuracy of the spacecraft orbits. Finally, the SISRE value used for the assessment of the clock products is found from the RMS of all SISREs computed for the individual satellites of the complete constellation.

Fig. 3 depicts the SISRE computed from the RETICLE orbit/clock-product for each satellite of the GPS constellation on 2008/08/20. The CODE final orbits and clocks have been used as a reference. Note that PRN 1 and PRN 5 are missing on this day, because they are set as unhealthy. The black bars indicate the orbit-only SISRE. Since RETICLE uses the ultra-rapid predicted orbits, the orbit-only SISRE reflects the accuracy of these orbits, and ranges between 2 cm and 6 cm for all satellites. The red bars on the other hand, show the total SISRE according to Eq. 10. The majority of the satellites has a SISRE smaller than 10 cm, however, five satellites have larger SISRE with up to 22 cm. If the variation of the SISREs for the complete constellation is observed over a longer time, it becomes obvious that satellites with a slightly increased values appear from time to time.

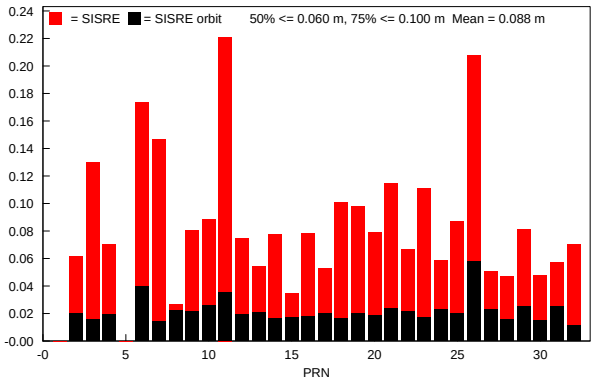

Fig. 3 Signal in Space Range Error of the RETICLE clock product on 2008/08/20, the black bars indicate the orbit-only SISRE, the red bars show the combined SISRE, the mean constellation SISRE is 8.8 cm

As already explained, Eq. 10 eliminates a common radial offset in the range error. Fig. 4 depicts the mean constellation offset, which has been removed during the SISRE computation in Fig. 3. It can be seen that the common offset for the RETICLE product on this particular day varies between 0.6 m (2 ns) and -1.4 m (4.3 ns). The most rapid variations occur between 10h and 11h and also between 22h and 23h. These variations result from the clock constraint, which is imposed by the RETICLE-system on the GPS clocks. As already explained, the mean of the estimated RETICLE clocks is constrained to the mean clock offset in the IGU predicted clocks, which are in turn tied to the GPS time scale. Therefore the variations of the mean clock in Fig. 4 correspond to the variations of the mean IGU predicted clock. It can be observed that the mean clock offset has only a small variation between 0h and 10h. The rapid change in the following hour results from the transition to the new, updated IGU orbit, which is released at 9h UTC and apparently has an offset of approximately 4 ns compared to the previous product. The mean clock drifts then slowly from -0.5 m to -1.4 m at 22 h, where a new IGU product change takes places in the filter. The additional delay of one hour in the change from one IGU product to the next one is caused by the filter. It is interesting to note that at 4h and 16h, where the IGU product is also changed, no apparent offset between the consecutive products exists.

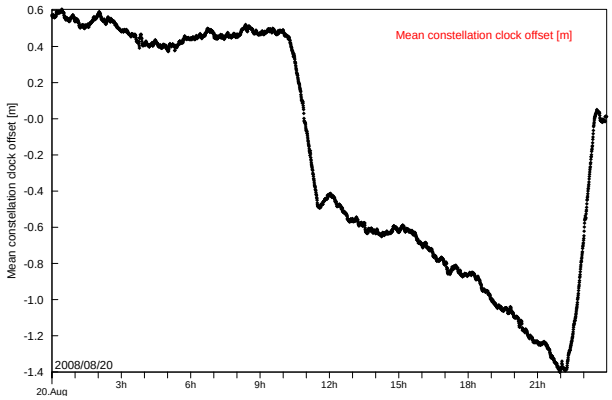

Fig. 4 Variation of the mean constellation clock offset of the RETICLE clock product for 2008/08/20, the rapid change results from the transition to a new ultra rapid predicted orbit

Complementary to the SISRE computation, the orbit and clock product has also been used in a LEO-satellite orbit determination. The POD-procedure is identical to the standard POD which is used in the operational processing at GSOC. An iterated least-squares estimator implemented in the GPS High Precision Orbit Determination Tools (GHOST) has been utilized for this analysis. This batch algorithm provides estimates of the satellites position and velocity, coefficients for the atmospheric drag and solar radiation pressure acting on the satellite, the receiver clock offset and the carrier phase ambiguities. Additionally, empirical accelerations are estimated which compensate unmodelled perturbation forces. The filter uses a reduced dynamical model for the satellites trajectory. In the following, this batch algorithm will be referred to as RDOD-tool

(Reduced-Dynamic Orbit Determination). A detailed description of the RDOD-algorithm can be found in [11].

PRECISE ORBIT DETERMINATION RESULTS

Real flight data of the satellite TerraSar-X has been used for the accuracy assessment of the RETICLE clock products. 15 consecutive days of data starting at 2008/08/18 (DoY 231) have been selected. In a first step, the SISRE for the two-week time interval has been computed according to the equations derived in the previous section. The results are presented in Fig. 5. It shows the SISREs for each day computed using CODE orbits and clocks as reference solution. Variations of approximately 5 cm can be observed around a mean of about 10 cm. On day 232, however, the SISRE is exceptionally high with 22.5 cm. At this day, the clock corrections of two satellites are affected by large offsets in the order of several decimeters with respect to the CODE solution. These offsets are probably due to undetected cycle-slips. According to these results a positioning accuracy at decimeter level would be expected for the RETICLE clock product.

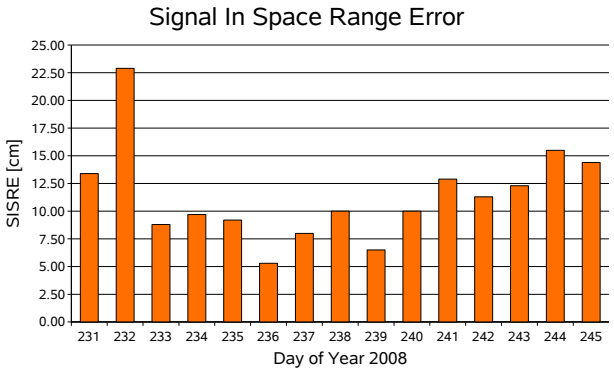

Fig. 5 Signal in Space Range Error for RETICLE results over a two week period

For the assessment of the POD results obtained with the RETICLE orbits and clocks, a reference solution for the TerraSar-X orbit is obtained using the CODE orbits and clocks at a rate of 30 seconds. The 3D position errors of the POD results using the real-time product are then computed with respect to this reference solution. Each day a 24h POD has been performed with RDOD. Fig. 6 shows the results for the RETICLE prodcuts and for the IGU predicted orbits and clocks. The position errors for RETICLE vary between approximately 2.5 cm and 6 cm. The positioning accuracy exceeds the expectations based on the SISRE computation shown in Fig. 5 for the entire time span. The positioning accuracy on day 232 is not significantly reduced compared to other days, despite the large SISRE for this day.

The explanation for the better accuracy of the positioning results is, that the orbit determination benefits from estimation of float ambiguities for the carrier phase measurements. Biases in the individual satellite clock corrections of the RETICLE products are absorbed into these ambiguities and do not affect the positioning accuracy as long as the clock correction accurately reflects the short term behavior of the GPS clock. The pseudorange measurements on the other hand are affected by biased clock correction values, but have a much lower weight in the orbit determination compared to the carrier phase observations. The SISRE computation does not account for the effect of carrier phase ambiguities and therefore reflects the total error in the clock offsets compared to the CODE reference solution.

The small variations in the positioning accuracy over the two week interval are most likely caused by a varying availability of the GPS reference stations. Furthermore, the clock estimation for individual satellites must be reinitialized after a satellite outage, a maneuver or a maintenance. The Kalman-filter requires some time until the clock offset estimation for the affected satellite has reached the same level of accuracy as the other satellites.

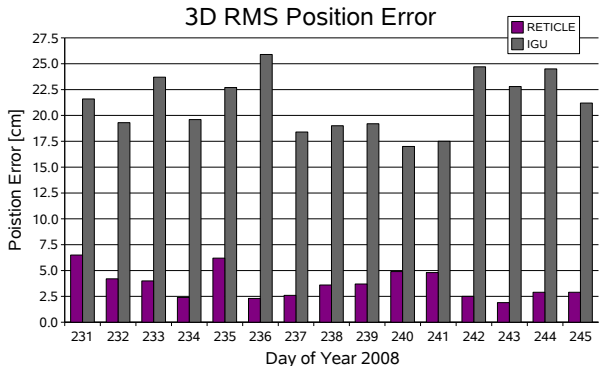

Fig. 6 3D RMS position errors for TerraSar-X using the RETICLE and IGU predicted product, the reference orbit for the comparison has been computed using CODE orbit and clocks

Fig. 6 additionally provides the results which have been obtained using the IGU predicted orbits, which contain predicted clocks and orbits at 15 minute epochs. This product is currently the only freely available product besides the broadcast ephemerides, which can be used for global real-time positioning. The plot shows that the 3D positioning errors vary between approximately 16 cm and 26 cm. It must be kept in mind that the RETICLE orbit and the IGU predicted orbits are identical. Thus the decrease in positioning accuracy is solely caused by the degraded accuracy of the predicted clock offsets.

The POD quality can also be assessed by analyzing the pseudorange and carrier phase measurement residuals. The residuals are computed as the RMS of all measurements residuals with respect to the orbit obtained from the RDOD algorithm. Measurements which have been rejected in the filter are not included in the residuals. The pseudorange residuals for the CODE product are approximately 75 cm and constant for each day. The pseudorange residuals of the RETICLE clock product have the same RMS value, except

for day 232 which exhibits increased pseudorange residuals of 82 cm. These increased residuals are another manifestation of the two biased clock offsets. The IGU product has significantly larger pseudorange residuals with approximately 1.1 m. The plot in Fig. 7 shows the RMS residuals of the carrier phase observations. Expectedly, the CODE product exhibits the smallest residuals of 4 mm, which is close to the receiver noise for the carrier phase measurements. It should be noted that empirical in-flight antenna phase pattern corrections have been applied to reduce the residuals to this level (see [12] for details). The RETICLE products has carrier phase residuals of 11 mm with a standard deviation of 2 mm. The largest residuals are again found for the IGU product with 32 mm $\pm$ 4 mm.

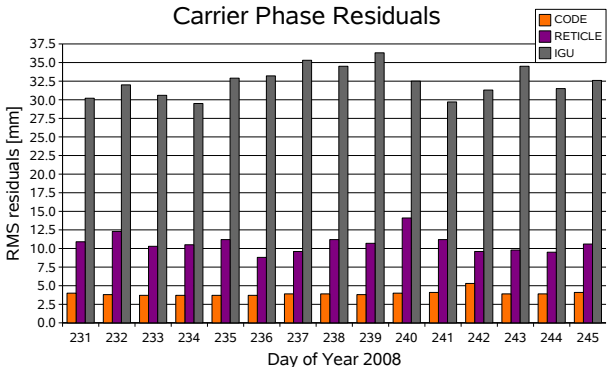

Fig. 7 Carrier phase residuals for TerraSar-X using CODE, RETICLE and IGU predicted orbits and clocks

The analysis of the measurement residuals offers another possibility to assess the quality of the different clock products. The carrierphase residuals of the CODE product are at the lowest possible level. The RETICLE residuals are larger and reveal the effect of remaining noise errors on the estimated clocks. It should be kept in mind, however, that the CODE product is produced using a batch estimator, which always produces more accurate results than a Kalman filter without forward/backward smoothing.

SUMMARY AND CONCLUSIONS

The paper has introduced the real-time clock estimation system RETICLE, which is currently established at GSOC. The core algorithm of the system is based on a Kalman-filter, which estimates globally valid clock offsets for the complete GPS constellation based on the IGU predicted orbits. The final products are satellite orbits and clocks at a rate of 30 seconds. The analysis with real flight data of the TerraSar-X has demonstrated that these orbit and high-rate clocks are well suited for near real-time precise orbit determination of low earth orbit satellites. The 3D position errors achieved with the RETICLE-product are well below a decimeter. With this performance, the near real-time POD requirements of current and future mission are fulfilled.

The signal in space range error has been used in the analysis to show a quick and convenient measure of the orbit and clock product quality. The accuracies achieved in the POD are, however, always higher as indicated by the SISRE, since the orbit determination benefits from the estimation of float carrier phase ambiguities, which absorb constant radial biases.

It has also been demonstrated that the current network of real-time GPS reference stations is sufficient for precise clock estimation. However, in areas with reduced coverage like the pacific and also Africa, a densification of the station network would certainly benefit the quality of the prodcuts. The challenge in working with real-time data streams lies in the varying latency and completeness of the global observations. Due to network connection issues, a certain fraction of the observation epochs is lost during transmission from the GPS station to the user. Unfortunately, especially stations in sparsely covered areas exhibit frequent outages of their data streams. These losses reduce the number of redundant measurements per GPS satellite even further.

A second problem which affects the completeness of the observations is the latency of the data. Usually all stations used for RETICLE have a latency of about 2 or 3 seconds. However, from time to time the latency increases for individual stations and as a results, the measurements arrive in the system after the measurement update has already been performed. Because of these issues, the amount of data available in real-time from a given station network is in general lower than the accumulated data obtained from daily Rinex-files for the same network. However, in comparison with post-processed clocks, obtained with an offline version of the RETICLE-filter, the real-time clocks do not show significant differences in the POD-performance [13]. It can therefore be summarized that the occasional data-losses in the real-time network do not significantly affect the clock estimation.

The configuration control of the NTRIP stations will be another challenge for the real-time community. Changes in the station hardware like receiver or antenna replacements and possibly also software updates must be announced to the user in order to allow consistent data processing. The IGS has established a configuration control for the tracking network, which is based on sitelog files, which are updated by the station operators when changes to the station configuration have been done. The sitelog information then migrates into the daily Sinex-files and is then conveniently available to users. However, for real-time processing the latency of this procedure is certainly too long. On the other hand, the information transmitted by the real-time stations in the RTCM2/3- or RTIGS-messages has been found to be unreliable as well. In many cases, the corresponding messages are not transmitted or incorrectly configured. A configuration control system, which distributes the necessary information reliably and quickly to the users, will certainly benefit to the quality of the real-time products.

REFERENCES

[1] Y. Bar-Sever, B. Bell, A. Dorsey, J. Srinivasan, "Space Applications of the NASA Global Differential GPS System", Institute of Navigation, Portland, Oregon, USA, 2003

[2] L. Agrotis, J. Dow, C-G. Martinez, A. Ballereau, J. Pérez, "Real Time GNSS Processing at ESOC: Infrastructure and Initial Results", IGS Workshop 2008, Miami, Florida, USA

[3] Weber G., Dettmering D., Gebhard H., "Networked Transport of RTCM via Internet Protocol (NTRIP)", In: Sanso F. (Ed.): "A Window on the Future, Proceedings of the IAG General Assembly", Sapporo, Japan, 2003, Springer Verlag, Symposia Series, Vol. 128, p. 60-64, 2005.

[4] S. Schaer, S. Steigenberger, "Determination and Use of GPS Differential Code Bias Values" IGS Workshop Darmstadt, Germany, 2006

[5] R. Schmid, P. Steigenberger, G. Gendt, M. Ge, M. Rothacher, "Generation of a consistent absolute phase center correction model for GPS receiver and satellite antennas", Journal of Geodesy, Vol. 81, No. 12, pp 781-798, 2007

[6] D.D. McCarthy, G. Petit, "IERS Technical Note No. 32 (2003)", Verlag des Bundesamts für Kartographie und Geodäsie, Frankfurt am Main, Germany, 2004

[7] P. Collins, R. Langley, J. LaMance, "Limiting Factors in Tropospheric Propagation Delay Error Modelling for GPS Airborne Navigation", Proceedings of The Institute of Navigation 52nd Annual Meeting, Cambridge, Massachusetts, June 19-21 1996, pp. 519-528, 1996

[8] J.T. Wu, S.C. Wu, G.A. Hajj, W.I. Bertiger, S.M. Lichten, "Effects of antenna orientation on GPS carrier phase", Manuscripta Geodaetica 18, pp. 9198, 1993

[9] S. Hutsell, "Relating the Hadamard variance to MCS Kalman filter clock estimation", 27th Annual Precise Time and Time Interval (PTTI) Applications and Planning Meeting, pp. 291-301, 1996

[10] D.L.M. Warren, J.F. Raquet, "Broadcast vs. Precise GPS Ephemerides: A Historical Perspective", GPS Solutions 7(3), 2003

[11] O. Montenbruck, T. van Helleputte, R. Kroes, E. Gill, "Reduced Dynamic Orbit Determination using GPS Code and Carrier Measurements",. Aerosp. Science and Technology 9/3, pp. 261-271

[12] O. Montenbruck, M. Garcia-Fernandez , Y. Yoon, S. Schn, A. Jggi, "Antenna Phase Center Calibration for Precise Positioning of LEO Satellites", GPS Solutions, June 2008

[13] A. Hauschild, "Kalman-Filter-Based GPS Clock Estimation for Near Real-time Positioning", submitted to GPS Solutions